

Effect of sealing with ultraviolet-curable adhesives on the performance of dye-sensitized solar cells

Tzu Hsuan Chiang, Chun Hsiung Chen, Chun Yu Liu

Department of Energy Engineering, National United University, 2, Lienda, Nan-Shi Li, Miaoli, Taiwan 36063, Republic of China

Correspondence to: T. H. Chiang (E-mail: thchiang@nuu.edu.tw)

ABSTRACT: In this study, we investigated different types of oligomers, including an aliphatic polyester-based urethane diacrylate (CN 991) and aliphatic hydrophobic backbone (CN 9014), and different contents of the oligomers and different amounts of 2-(perfluorohexyl) ethyl methacrylate (PFE) monomer in ultraviolet (UV)-curable adhesive to explore the effects of their resistance to corrosion on the basis of the electrolyte, adhesion strength, and performance of the sealing of dye-sensitized solar cells (DSSCs). The DSSCs were sealed with a 58% CN 9014 containing UV-curable adhesive mixed with 3.0 wt % PFE monomer, which had the greatest open-circuit voltage and short-circuit current density. A 4.8% efficiency was obtained after the sample underwent long-term thermal stability tests at 60°C for 37 days. The performance of the 3.0 wt % PFE-containing UV-curable adhesive in the sealing of DSSCs was better than that of Surlyn for long-term thermal stability. In addition, this adhesive provided better resistance to corrosion because of the electrolyte and enhanced the DSSCs' durability. © 2015 Wiley Periodicals, Inc. *J. Appl. Polym. Sci.* **2015**, *132*, 42015.

KEYWORDS: applications; morphology; packaging; properties and characterization

Received 14 August 2014; accepted 19 January 2015

DOI: 10.1002/app.42015

INTRODUCTION

Dye-sensitized solar cells (DSSCs), first identified in 1991, are new inventions in thin films developed by Oregan and Grätzel.¹ They are made of low-cost materials and are cheaper to manufacture than silicon and copper indium gallium selenide solar cells. Because of the dye used, DSSCs can absorb both diffused sunlight and fluorescent light. Therefore, DSSCs have a very low cutoff that can work in cloudy weather, non-direct sunlight, and low-light conditions (e.g., indoor).² DSSCs have a higher power density across indoor conditions,³ large-area applications that are light in weight,⁴ and a display of different colors depending on the use of different dyes⁵ relative to amorphous silicon and organic solar materials solar cells. During the past few years, DSSCs have been developed to be flexible on plastic substrates, such as indium tin oxide coated poly(ethylene naphthalate) film,⁶ poly(ethylene naphthalate) film,⁷ and a titanium or titanium alloy, such as Ti-6Al-4V (The chemical composition consist of 6% aluminium, 4% vanadium, 0.25% (maximum) iron, 0.2% (maximum) oxygen, and the remainder titanium).^{8–10} However, such substrates are more disadvantageous than glass substrates. For example, plastic substrates used for DSSCs were limited because the working electrode used as the titanium dioxide (TiO₂) layer needed sintering at 400°C, and the plastic substrates readily produced thermal degradation and outgas. They also had poorer water and gas resistance, which could cause damage to the dye. The

metal substrates were possibly corroded by the iodide/triiodide redox couple, which is a crucial part of the liquid electrolyte and is chemically aggressive toward many metals.¹¹ Although the glass substrates have a lower coefficient of thermal expansion than adhesives, the DSSC devices could be used in an indoor environment in the future, this difference in the coefficient of thermal expansion could be neglected. Therefore, today, glass substrates are still widely used in DSSCs.

In addition, the electrolytes of DSSCs consist of high-polarity organic solvents, iodides, and additives.¹² The choice of organic solvents depends on the required cell performance. The use of highly polar solvents, such as acetonitrile, *N*-methyl pyrrolidone, 3-methoxypropionitrile, poly(vinyl carbonate), γ -butyrolactone, and ethylene carbonate,¹³ causes the electrolyte to have a higher thermal expansion coefficient than fluorine-doped tin oxide (FTO) glass, which forms cracks between the sealing agents and the FTO glass during higher temperature operations. In addition, highly polar solvents can easily corrode adhesives; this causes electrolyte leakage and reacts with the silver current collectors of DSSC modules,² changing the electrolyte components¹⁴ during long-term operations. Therefore, the design of the chemical structure of the adhesive is important, as it is hard to corrode the polar solvent and iodine to prevent the leakage of iodide from the cell.

In the past, Surlyn has been used as a DSSC sealant as it is functional up to a temperature of 120°C.¹⁵ Some studies have

used glass frits¹⁶ sintered at temperatures ranging from 580 to 650°C. Because of the high operational temperatures of these sealants, the quality of the dye adsorbed onto the TiO₂ electrode was negatively affected; this caused a desorption or deterioration of the dye and a reduction in the efficiency of the DSSC. Therefore, some researchers, such as Hinsch *et al.*,² used an ultraviolet (UV) adhesive in DSSC, whereas Lee *et al.*¹⁷ used UV glue for the sealed injection holes and the edge of the DSSC and a UV-curable adhesive in the DSSC module to bond the upper and lower transparent substrates to each other while simultaneously insulating the film between the unit electrodes.¹⁸ UV-curable adhesives offer several advantages, including fast curing and room-temperature curing, high thermal stability, and excellent adhesion. However, the adhesives used for sealing in DSSCs cause the DSSCs to have a short lifetime when they are subjected to long-term operations. Three Bond was the first to use UV-curable adhesives for sealing DSSCs.¹⁹ They produced 31X-101, which has high electrolytic resistance properties, and applied it to the periphery of the gap between the two substrates for DSSCs.²⁰ However, the high costs involved meant that it was not well accepted in the market.

Thus far, few research activities have focused on only those sealant materials that allow DSSCs to achieve high conversion efficiencies in long-term thermal stability tests. To overcome DSSCs' short lifetime problem, in this study, we investigated the use of a fluorine polymer, 2-(perfluorohexyl) ethyl methacrylate (PFE), added to a UV-curable adhesive to enhance the resistance to corrosion by electrolytes. Fluorine polymers have an extremely strong carbon-fluorine bond and an impermeable sheath of fluorine atoms surrounding the carbon-carbon chain. They, thereby, provide excellent chemical and solvent resistance.²¹ They can also greatly enhance the flame resistance, durability, thermal stability, photostability, low surface energy, low coefficient of friction, and weatherability.^{22,23} Therefore, the increased content of the fluorine monomer enhanced the chemical resistance of the polymer. In this study, we used a PFE monomer because it had 13 fluorine groups and could provide a lot of resistance for the solvent. In this study, we investigated different types and contents of oligomer in UV-curable adhesives; this affected resistance to corrosion by the electrolyte and the adhesion strength of the FTO glass. We also investigated different amounts of the fluorine polymer PFE, a substance that affects resistance to corrosion by electrolytes.

EXPERIMENTAL

Preparation of UV-Curable Adhesives and Electrolytes

The UV-curable adhesive consisted of an oligomer with different amounts of an aliphatic hydrophobic backbone (CN 9014) or an aliphatic polyester-based urethane diacrylate (CN 991) purchased from Sartomer. A 9.0 wt % photoinitiator, 2-methyl-4'-(methylthio)-2-morpholinopropiophenone, was purchased from Tokyo Chemical Industry Co., Ltd. A 9.0 wt % acrylic acid was purchased from Acros Organics, and a 24.0 wt % acrylic acid isobornyl ester was purchased from Tokyo Chemical Industry Co., Ltd. After all of the materials were mixed together, the mixture was stirred for 1 h at room temperature.

The fluorine-containing UV-curable adhesives were prepared with different amounts (i.e., 0.5, 1.0, 1.5, and 3.0 wt %) of PFE

purchased from Aldrich; each amount was mixed with the blank adhesive and then stirred for 2 h at room temperature.

The electrolyte consisted of 0.8M 1-propyl-3-methylimidazolium, 0.1M iodine (I₂), and 0.5M *N*-methyl benzimidazole in 3-methoxypropionitrile. All of the ingredients were purchased from Acros Organics.

Fabrication of the DSSCs

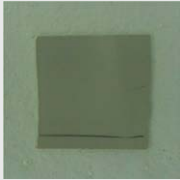
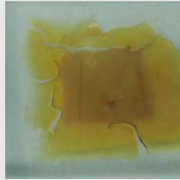


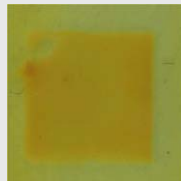
The FTO-conductive glass (15 Ω/□, Ruilong Co., Inc., Taiwan) was cleaned in acetone and ethanol (Aldrich) with an ultrasonic cleaner. Commercial nanocrystalline TiO₂ (P25, Degussa) and poly(ethylene glycol)-*block*-poly(propylene glycol)-*block*-poly(ethylene glycol) (P123, Aldrich) were mixed in *n*-butanol (Aldrich) to form a colloidal suspension of TiO₂. A TiO₂ layer (~10 μm) was subsequently prepared with the doctor blade coating technique on the FTO glass, after which it was sintered at 400°C for 1 h. After cooling, the TiO₂ electrode was treated further by a 40 mM aqueous solution of titanium tetrachloride (Aldrich) at 70°C for 30 min and then calcined at 400°C for 1 h. After calcining and once the temperature had cooled to 80°C, the TiO₂ electrode was immersed in a ruthenium dye [ditetrabutyl ammonium *cis*-bis(isothiocyanato)bis(2,2'-bipyridyl-4,4'-dicarboxylato) ruthenium(II), N719, Aldrich] solution (0.5 mM N719 in ethanol) for 24 h in the dark. The excess dye was rinsed off with ethanol. The ion-sputtering method was used to deposit a thin layer of Pt on another FTO glass substrate, and this served as the cathode. The four sides of two electrodes (main sealing) were sealed with a 25-μm thick Surlyn film (DuPont) at 110°C for 30 s or used with UV-curable adhesives exposed to UV irradiation for 15 s (1 kW of UV light source, 80 W/cm of UV intensity). The distance between the sample and the UV light lamp was 15 cm. The electrolyte solution was then added through one of the two holes that had been drilled in the counter electrode. Both holes (made for end sealing) were then immediately sealed with Surlyn film or UV-curable adhesives between the cathode substrate and a microscope slide.

Characteristics of UV-Curable Adhesive Analysis

The hardness of the UV-curable adhesives was measured with a pencil scratch hardness tester (PPH-1000, Chuanhua, Taiwan), and the process corresponded to the ASTM D 3363 standard. The surface morphologies and corrosion images of the cured adhesives were analyzed via scanning electron microscopy (SEM) with a JEOL JED 2300 instrument and recorded with a Nikon Coolpix P310 digital camera.

The UV-curable adhesive was applied between the 1 × 1 cm² FTO glass plates to form the pull test specimen. The specimens were cured in a UV oven (KN-10K1, Kuang Neng Co., Ltd., Taiwan) with wavelengths ranging from 254 to 390 nm. The distance between the sample and the UV light lamp was 15 cm under a power of 80 W/cm for irradiation for 15 s to complete the curing process. Two steel bars were then attached to the two ends of the sample and connected to a pull tester for adhesion strength measurement at a pull rate of 20 mm/min. The pull tester was a model AI-7000-S instrument purchased from Gotech Testing Machines, Inc. (Taiwan). For each type of adhesive sample, the pull test was repeated five times. The adhesion

Table I. Corrosion Images of Different Oligomer Types of UV-Curable Adhesives in an Electrolyte. [Color table can be viewed in the online issue, which is available at wileyonlinelibrary.com.]

Soaking time in electrolyte	Without soaking	First day	Second day
CN 991 containing UV-curable adhesive			—
Corrosion percentage (%)	0	100	—
CN 9014 containing UV-curable adhesive			
Corrosion percentage (%)	0	63.0	100

strengths of the adhesive resins were measured with a pull tester, which adhered to the ASTM D 897 standard.

The surface energy (γ) was measured with a surface tension instrument (FTA-1000D) from First Ten Angstrom, Inc. Receding contact angles were measured by a 9- μ L water drop on the cured UV-curable adhesives; the drop was placed on the surface of the sample for 10 s. On the basis of the Girifalco–Good–Fowkes–Young (GGFY) method, the surface energy was computed with eqs. (1) and (2):²⁴

$$\cos \theta = -1 + \frac{2\sqrt{\gamma_{sv} + \gamma_{LV}}}{\gamma_{LV}} \quad (1)$$

$$\gamma_{sv} = \text{total } \gamma \quad (2)$$

where θ is the contact angle, measured in degrees; γ_{sv} is the surface tension between the solid and vapor; and γ_{LV} is the surface tension between the liquid and vapor.

Characterization of the Long-Term Thermal Stability of the DSSCs

The long-term thermal stability test involved the placement of the DSSCs into an oven at 60°C for 37 days. After the test was completed, the photovoltaic parameters—namely, the current–voltage—of the DSSCs were measured. The current–voltage characterization was performed with a Keithley 2400 source meter provided by an Oriol solar simulator (model 91192, Newport Corp.). The conversion efficiency (η) of the solar cells was calculated as the ratio between the maximum power (P_m) generated by a solar cell and the incident power (P_{in}). The incident power was equal to the irradiance of the AM 1.5 spectrum normalized to 1000 W/m². η was determined from the current–voltage measurement with eq. (3):²⁵

$$\eta = \frac{P_{mt}}{P_{in}} \times 100 = \frac{J_{SC} V_{OC} FF}{P_{in}} \times 100 \quad (3)$$

where the J_{SC} is the short-circuit current density, V_{OC} is the open-circuit voltage, and FF is the fill factor. FF was determined by the ratio of the maximum obtainable power to the theoretic-

cal obtainable power, where the latter was the product J_{SC} . In addition, the efficiency degradation of the DSSC device was calculated with eq. (4):

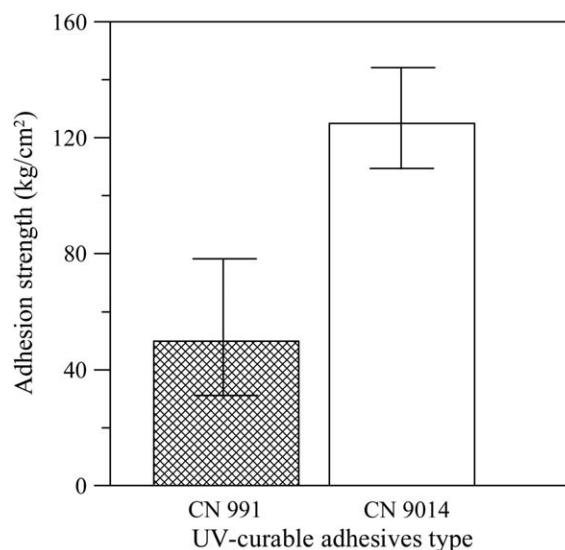
$$\text{Efficiency degradation (\%)} = \frac{\eta_0 - \eta_n}{\eta_0} \times 100 \quad (4)$$

where η_0 is the original conversion efficiency of the DSSC device and η_n is the conversion efficiency of the DSSC device undergoing a long-term thermal stability test for 37 days.

RESULTS AND DISCUSSION

Effect of the Oligomer Type and Content on the Resistance to Corrosion by the Electrolyte

The UV-curable adhesives were prepared with 29.00 wt % CN 991 and 29.00 wt % CN 9014 resin as oligomers. The two UV-curable adhesives were glued on 1 × 1 cm² cured silver adhesives (which were previously coated on FTO glass). Then, the

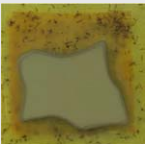
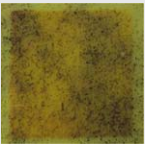


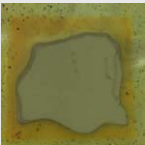




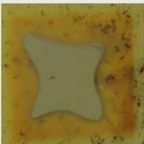
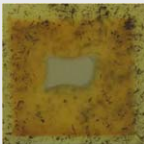
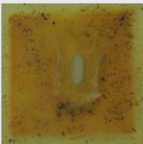

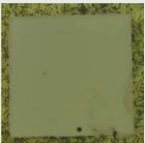
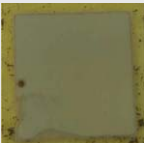
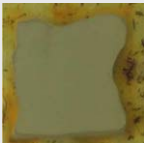

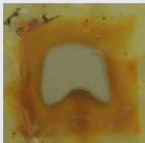
**Figure 1.** Adhesion strength of CN 991 and CN 9014 containing UV-curable adhesives for FTO glass.

samples were soaked in 10 mL of the electrolytes and kept at a temperature of 60°C. This experimental method can rapidly measure resistance to corrosion by the electrolyte of the UV-curable adhesives because of the silver ions' ability to readily react to iodine in the form of silver iodide (AgI).²⁶ The UV-curable adhesives' good protection against corrosion in the electrolytes could help the silver not to react to the iodine. Table I shows the ability of the two UV-curable adhesives to resist corrosion by the electrolytes. The results obtained show that the CN 9014 containing UV-curable adhesive had better resistance to corrosion by the electrolyte than the CN 991 containing UV-curable adhesive. The cured CN 991-containing UV-curable adhesive was soaked in electrolytes for 1 day, and the adhesive produced swelling, which caused cracking. The electrolyte-corrosion percentage of the CN 991 containing UV-curable adhesive was 100%, which was higher than that of the CN 9014 containing UV-curable adhesive (corrosion percentage = 63.0%), as shown in Table I. The main reason was that the two acrylate groups on the CN 991 oligomer structure had a higher crosslinking density when the adhesives were subjected to photopolymerization; this caused the cured adhesives to have a higher

hardness (hardness = 6H). The higher hardness adhesives easily created cracking, as the electrolytes formed vapor pressure and the incursive into the adhesive caused adhesive swelling. This situation caused the iodine of the electrolyte penetration, which reacted to the silver of the cured silver adhesive to disappear. The cured CN 991 containing UV-curable adhesive also had poor adhesion to the FTO glass, as shown in Figure 1; this allowed the electrolytes to permeate easily into the CN 991 containing UV-curable adhesive. However, the chemical structure of the CN 9014 containing UV-curable adhesive included one acrylate group with a lower crosslinking density and softness (hardness = 4B) of the cured adhesive. These properties of the provided adhesives did not easily create cracking because the adhesive had some flexibility, which reduced cracking by evaporating the pressure of the electrolytes in the 60°C environment. In addition, the cured CN 9014 containing UV-curable adhesive had good adhesion for the FTO glass, as shown in Figure 1. This helped the CN 9014 containing UV-curable adhesive have a better ability to resist corrosion.

As the CN 9014 containing UV-curable adhesive had better resistance to corrosion by the electrolyte than the CN 991 containing

Table II. Corrosion Images of Different Oligomer Contents in UV-Curable Adhesives in an Electrolyte. [Color table can be viewed in the online issue, which is available at wileyonlinelibrary.com.]

Soaking time in electrolyte	First day	Second day	Third day	Fourth day	Fifth day	Eighth day
19.14 wt % CN 9014			—	—	—	—
Corrosion (%)	62.0	100	—	—	—	—
29.00 wt % CN 9014			—	—	—	—
Corrosion (%)	61.0	100	—	—	—	—
38.28 wt % CN 9014				—	—	—
Corrosion (%)	50.5	96.0	100	—	—	—
48.72 wt % CN 9014						—
Corrosion (%)	0	50.5	70.0	92.0	98.3	—
58.00 wt % CN 9014						
Corrosion (%)	0	2.5	4.0	36.0	47.0	81.5

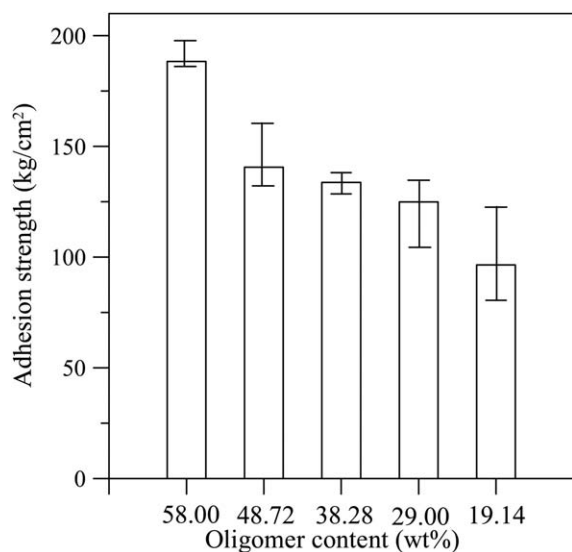


Figure 2. Adhesion strength of the oligomer with different contents of the UV-curable adhesive for FTO glass.

UV-curable adhesive, in the study, we investigated the influence of resistance to corrosion by the electrolyte for different content amounts of the CN 9014 oligomer. The UV-curable adhesives were added and had a range of different contents of CN 9014 oligomers—namely, 19.14, 29.00, 33.28, 48.72, and 58.00 wt %. The samples of UV-curable adhesives, each with different oligomer contents, were glued on $1 \times 1 \text{ cm}^2$ cured silver adhesives (which had previously been coated on FTO glass), and the samples were then soaked in 10 mL of electrolytes. The different levels of resistance to corrosion of the different UV-curable adhesives are shown in Table II. The results obtained show that the 19.14 and 29.00 wt % of the CN 9014 oligomer content in UV-curable adhesives had a poor ability to resist corrosion; their elec-

trolyte corrosion percentage was 100%, and the silver of the silver paste was dispersed with only 1 day of soaking time. When the CN 9014 oligomer content was increased to more than 29.00 wt % (i.e., 38.28 and 48.72 wt %), the cured adhesives showed an increased ability to resist corrosion (electrolyte corrosion percentage = 96.0 and 50.5% for 1 day of soaking time). The CN 9014 oligomer content of the UV-curable adhesives with 58.00 wt % demonstrated the largest resistance to corrosion. The electrolyte corrosion percentage was 2.5% for 1 day of soaking time. The silver paste remained on the FTO glass, and the electrolyte corrosion percentage was 81.5% after the adhesives were soaked in electrolytes for 8 days.

In addition, Figure 2 shows the adhesion strength of the UV-curable adhesive for FTO glass at different amounts of CN 9014 oligomer. When the CN 9014 oligomer content was decreased, the adhesion strength for FTO glass decreased. In the case of the lower CN 9014 oligomer content, the relative amounts of acrylic monomer increased in the adhesives, and the hardness of adhesives after exposure increased; this produced poor adhesion strength for the FTO glass.²⁷ This poor adhesion could have been due to the cured adhesives' poor resistance to corrosion by the electrolyte. In addition, as previously mentioned, harder adhesives easily created cracking when the electrolytes' incursion into the adhesive caused adhesive swelling; this was also likely to occur.

Effect of Different Contents of PFE Prepared in UV-Curable Adhesives on the Resistance to Corrosion by the Electrolytes

In this study, we further investigated the influence of efficiencies of DSSCs with blank UV-curable adhesives with different PFE monomer contents (i.e., 0.5, 1.0, 1.5, and 3.0 wt %). The different PFE monomer contents of UV-curable adhesives were coated on FTO conductive glass, after which the samples were then

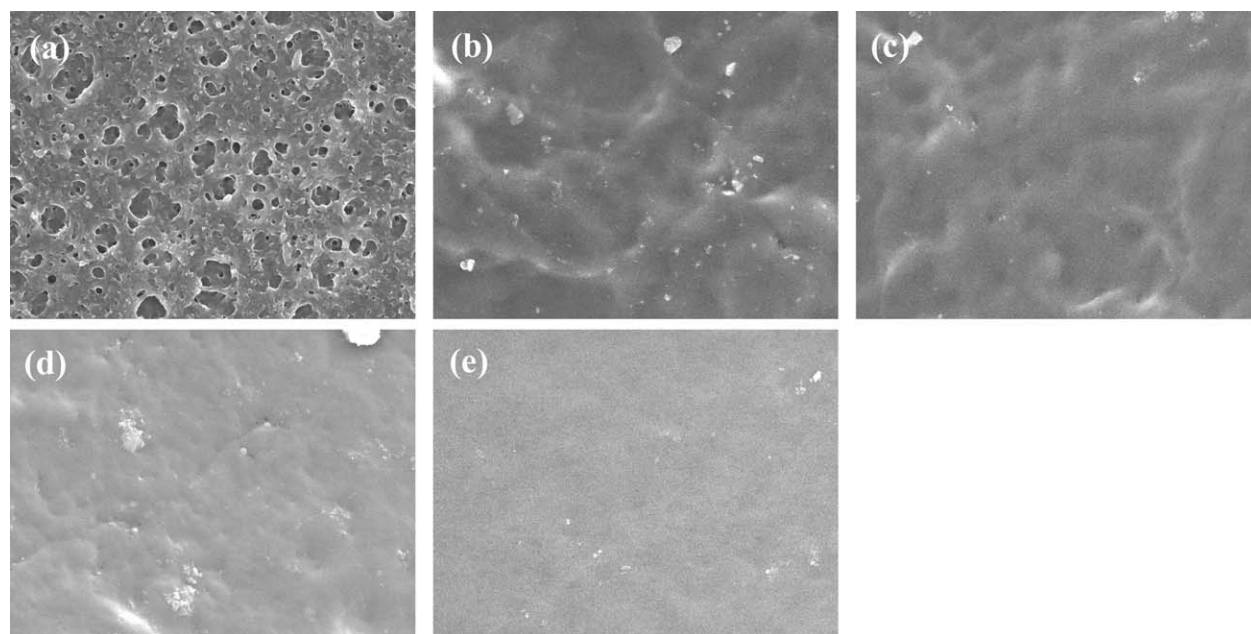


Figure 3. SEM images of the PFE-containing UV-curable adhesive with different PFE monomer contents: (a) blank, (b) 0.5 wt %, (c) 1.0 wt %, (d) 1.5 wt %, and (e) 3.0 wt %.

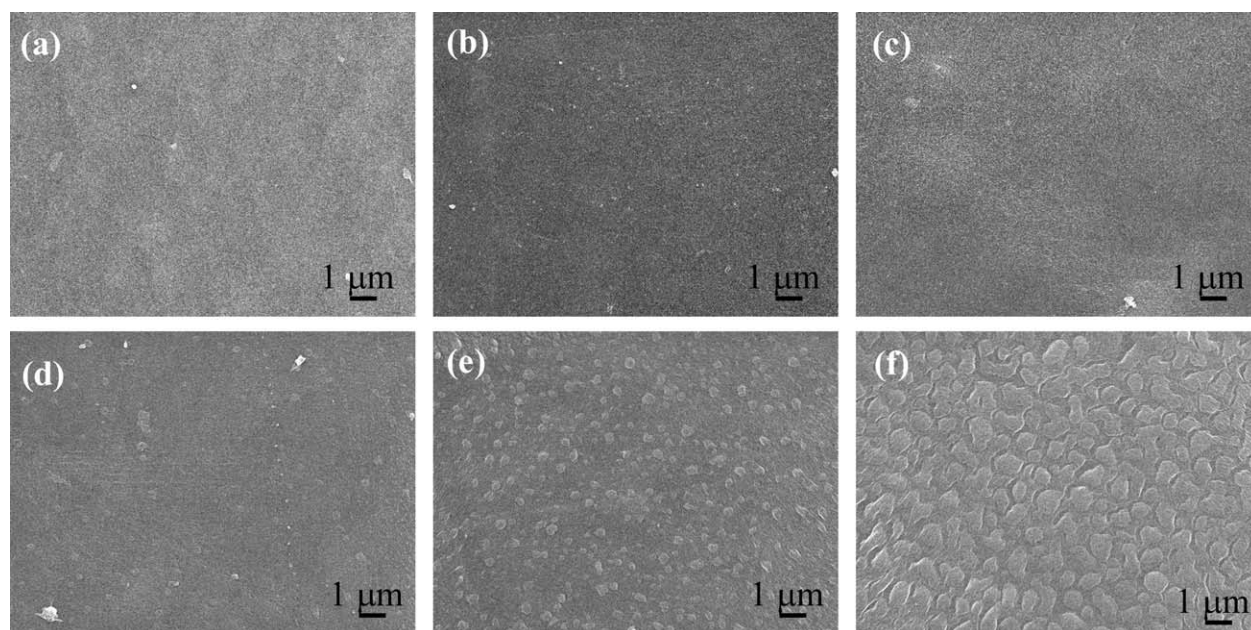


Figure 4. SEM images of Surlyn soaked in an electrolyte for (a) 5, (b) 15, (c) 20, (d) 25, (e) 30, and (f) 37 days.

subjected to irradiation for 15 s by UV light and soaked in the electrolyte at 60°C for 37 days. Figure 3(a) shows the SEM images of the cured blank adhesive, which became quite porous; this indicated that the cured blank adhesive was significantly corroded by the electrolyte. The results obtained by the cured blank adhesive show poorer resistance to the corroded electrolyte than to Surlyn, as shown in Figure 4. Therefore, the blank adhesive was added to 0.5–3.0 wt % PFE monomer; the SEM images of the cured adhesive during soaking in the electrolytes at 60°C for 37 days are shown in Figure 3(b–e). The results obtained from the blank adhesive contents of 0.5 and 1.0 wt % PFE monomer showed that some folds in the surface of the cured adhesives were corroded by the electrolytes. When the blank adhesive contained 3.0 wt % PFE monomer, the surface of the cured adhesive was smooth and not porous; this indicated sufficient resistance to the corroding electrolytes. As the PFE monomer had 13 fluorine groups, it was important to determine which adhesives contained a sufficient amount to enhance the adhesives' resistance to corrosion by the electrolytes. Therefore, the blank adhesives were selected to contain more PFE monomer to increase the resistance to corrosion by the electrolytes.

In addition, the PFE monomer content was increased in the blank adhesive, whose contact angles were increased and surface energies decreased, as shown in Table III and Figure 5. The

Table III. Surface Energy of Cured UV-Curable Adhesives with Different PFE Monomer Contents

PFE (wt %)	Surface energy (mJ/m ²)	Contact angle (°)
Blank	22.11 ± 0.25	83.69 ± 0.25
0.5	20.78 ± 0.20	85.64 ± 0.20
1.0	19.58 ± 0.47	86.32 ± 0.47
1.5	15.47 ± 0.35	87.46 ± 0.35
3.0	13.72 ± 0.30	94.11 ± 0.30

water contact angle of the cured blank adhesive was 83.69°. When 3 wt % PFE in the blank adhesive had the highest contact angle of 94.11°, the surface energy was computed with eqs. (1) and (2), and we obtained a value of 13.72 mJ/m²; this was lower than that of the blank adhesive (22.11 mJ/m²). The PFE monomer included 13 fluorine groups; these hydrophobic groups made the water have poor wettability and, thereby, caused the water to have a high contact angle. Therefore, when the PFE monomer in the blank adhesives was increased, the lower intermolecular interactions typically resulted in lower surface energies than found in the blank adhesives. In addition, Leadley *et al.*²⁸ reported that fluorinated siloxanes have a low surface energy and good solvent resistance. Therefore, the 3.0 wt % PFE UV-curable adhesive had a lower surface energy, and this led to better resistance to corrosion by the electrolytes.

As commercial Surlyn is commonly used in DSSC sealants, it is important to discuss the effects of Surlyn corrosion by electrolytes. The Surlyn was soaked in the electrolytes for different periods of time (i.e., 5, 15, 20, 25, 30, and 37 days) at a temperature of 60°C; the SEM images are shown in Figure 4. The results obtained show that the Surlyn made a few protrusions after soaking for 25 days. Thus, the Surlyn began to be corroded by the electrolytes. When the Surlyn soaking time was increased to 30 days, the surface of the Surlyn formed more protrusions. After we soaked for 35 days, the surface of the Surlyn showed the most protrusions; this indicated that Surlyn had been extensively corroded by the electrolytes. Therefore, Surlyn cannot serve as a long-term seal for DSSCs.

Photovoltaic Parameters of the DSSCs with Different PFE Contents

The photovoltaic parameters of the DSSCs for different PFE contents obtained with eq. (1) are shown in Figure 6. The V_{OC} , J_{SC} , and η values increased as the PFE monomer content increased in UV-curable adhesives when the DSSCs were

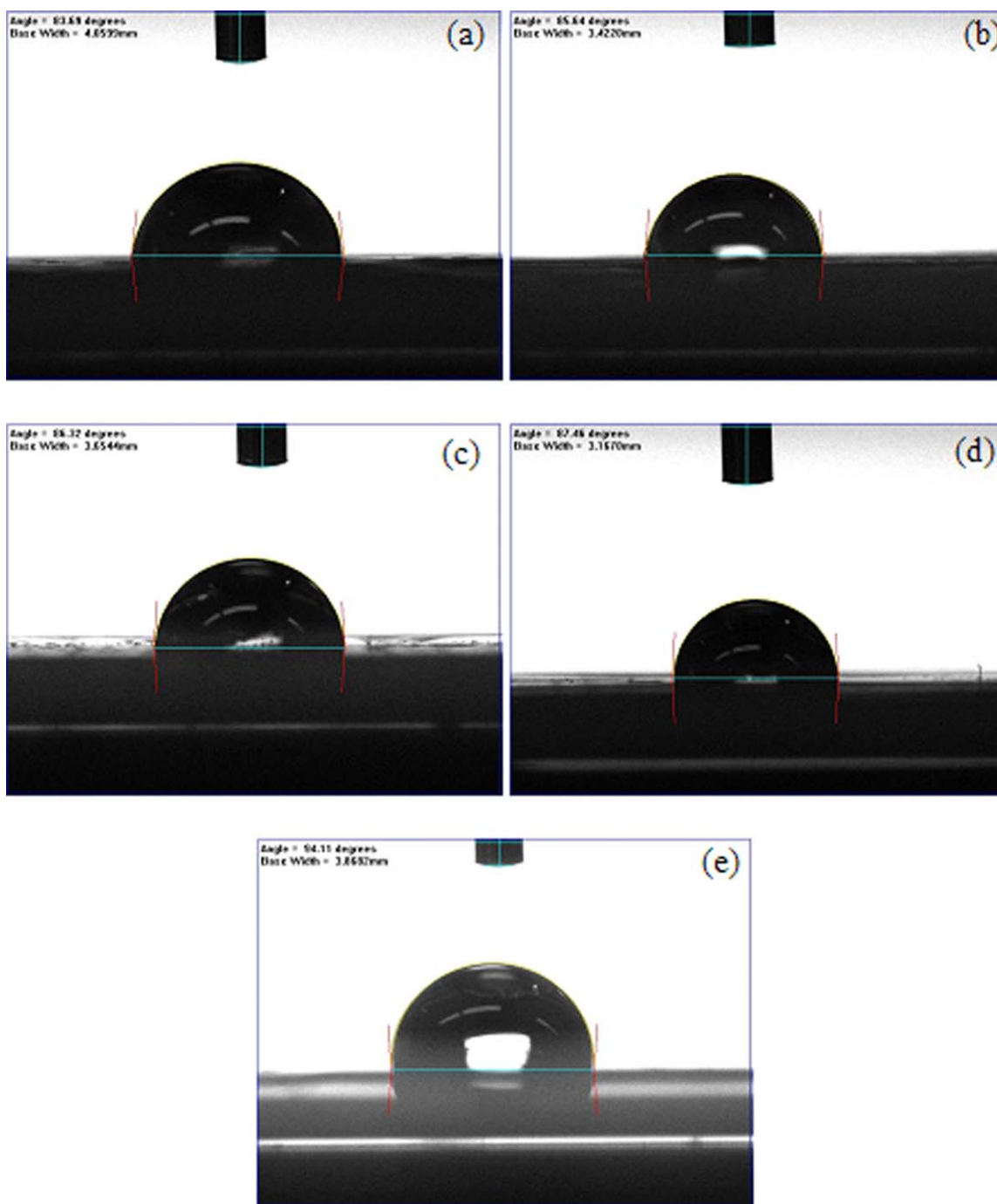


Figure 5. Contact angle images of the PFE-containing UV-curable adhesive with different PFE monomer contents: (a) blank, (b) 0.5 wt %, (c) 1.0 wt %, (d) 1.5 wt %, and (e) 3.0 wt %. [Color figure can be viewed in the online issue, which is available at wileyonlinelibrary.com.]

subjected to long-term thermal stability for 37 days. This result was also demonstrated by the SEM images in Figure 3. The samples offered sufficient resistance to the corrosive electrolytes: Fewer electrolytes reacted with the cured adhesives and resulted in few changes to the electrolyte components, and the relatively greater amounts of electrolytes proceeded to redox in the DSSCs, and this produced higher V_{OC} , J_{SC} , and η values.

To compare DSSCs' photovoltaic parameters, the DSSCs were sealed with Surllyn and 3.0 wt % PFE-containing UV-curable

adhesive, as shown Table IV. The four sides of the two electrodes (main sealing) and the two holes (drilled in the counter electrode) were sealed with Surllyn and 3.0 wt % PFE-containing UV-curable adhesive, respectively. The photovoltaic parameters of the DSSCs were subjected to long-term thermal stability tests (lasting 37 days). The tests yielded a cell efficiency of 4.8% and a degradation efficiency of 16.0% for the DSSCs sealed by the 3.0 wt % PFE-containing UV-curable adhesive. This was better than the results of the DSSCs sealed by Surllyn (efficiency = 4.0% and degradation

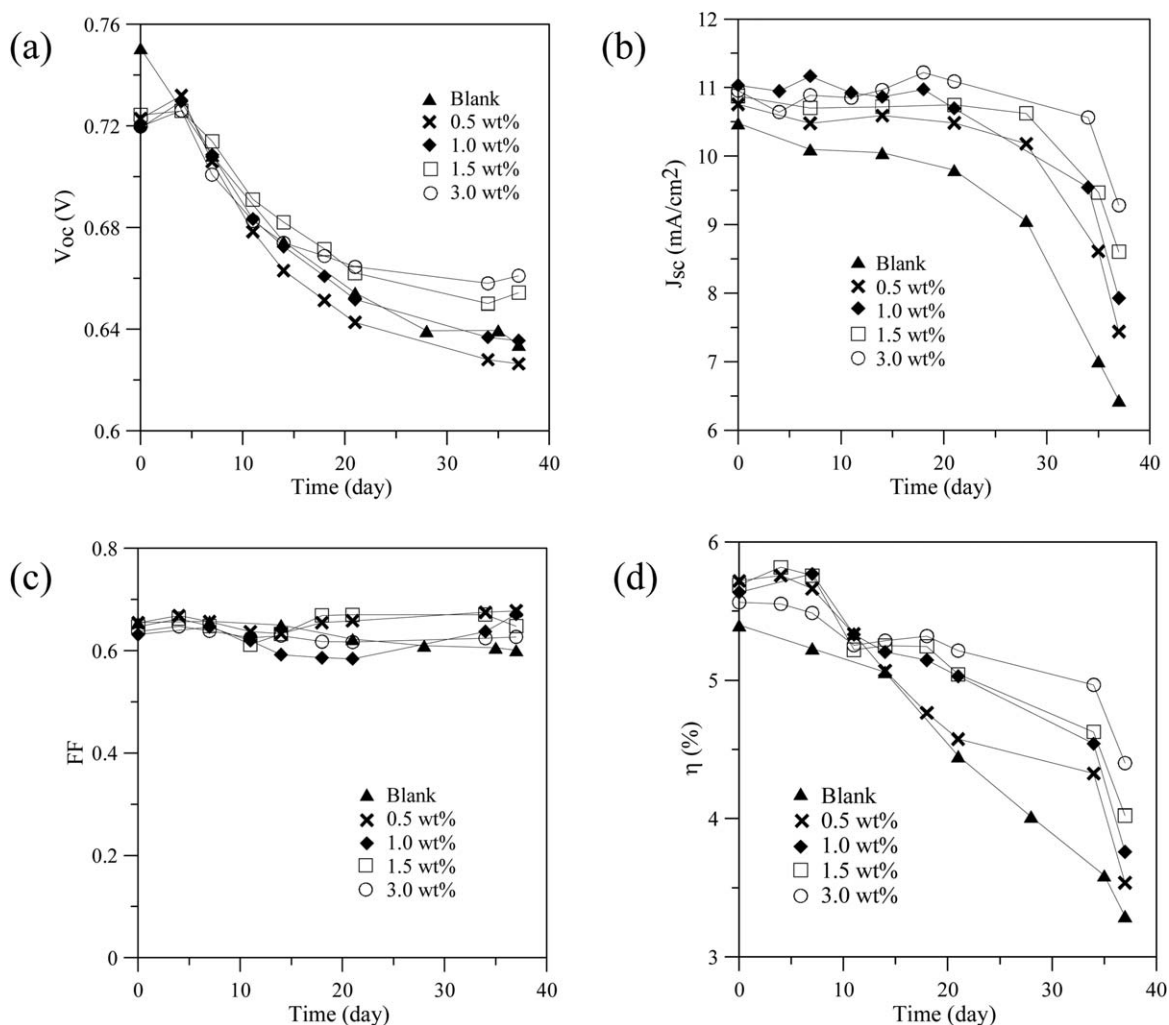


Figure 6. (a) V_{OC} , (b) J_{SC} , (c) FF, and (d) efficiency of DSSCs with different PFE monomer contents.

efficiency = 22.0%), as shown in Table IV. These results indicate that the use of PFM-containing UV-curable adhesive as the sealant for the DSSCs enhanced their resistance to the corrosive effects of the electrolytes and their durability. Although the blank adhesive containing 3.0 wt % PFE monomer had a better efficiency than Surlyn in the long-term thermal test. The conversion efficiency of this adhesive still decreased when the length of the long-term thermal test increased; this showed the limit of resistance to corrosion by the electrolytes. In the future, seal adhesives for DSSCs will be able to synthesize UV-curable fluorosilicone rubber, and this could provide better elasticity and resistance to corrosion by electrolytes.

CONCLUSIONS

In this study, the PFE monomer was added to the UV-curable adhesive for the sealing of DSSCs to provide better resistance to corrosion by the electrolytes and enhance DSSCs' durability. Adhesives with more hardness easily created cracking because of the electrolytes' incursion into the adhesive; this caused adhesive swelling and thereby caused the iodine of the electrolyte penetration that reacted to the silver of the cured silver adhesive to disappear. In addition, the PFE monomer content of the UV-curable adhesives increased, and this produced a lower surface energy and a better resistance to corrosion by the electrolytes. This caused the V_{OC} , J_{SC} , and η values of DSSCs to

Table IV. Photovoltaic Parameters for DSSCs Sealed with Surlyn and a PFE-Containing UV-Curable Adhesive After 37-Day, Long-Term Thermal Stability Tests

Sealant material	V_{OC} (V)	J_{SC} (mA/cm ²)	FF	η (%)	Degradation efficiency (%)
Surlyn	0.66 ± 0.05	9.12 ± 0.2	0.67 ± 0.06	4.0 ± 0.7	22.0 ± 0.7
PFE-containing UV-curable adhesive	0.68 ± 0.07	10.80 ± 0.1	0.69 ± 0.04	4.8 ± 0.5	16.0 ± 0.5

increase. The results obtained show that the cured 3.0 wt % PFE-containing UV-curable adhesive effectively sealed the DSSCs and provided greater values of V_{OC} , J_{SC} and η than Surlyn did.

ACKNOWLEDGMENTS

The authors thank the Industrial Technology Research Institute of Taiwan for providing analyses of the long-term thermal stability of the DSSC support for this research.

REFERENCES

1. Oregan, B.; Grätzel, M. *Nature* **1991**, 353, 737.
2. Hirsch, A.; Veurman, W.; Brandt, H.; Aguirre, R. L.; Bialecha, K.; Jensen, K. F. Presented at the 26th European Photovoltaic Solar Energy Conference and Exhibition, Hamburg, Germany, Sept **2011**.
3. Sridhar, N.; Freeman, D. Presented at the 26th European Photovoltaic Solar Energy Conference and Exhibition, Hamburg, Germany, Sept **2011**.
4. Kim, H. J.; Bin, Y. T.; Karthick, S. N.; Hemalatha, K. V.; Raj, C. J.; Venkatesan, S.; Park, S.; Vijayakumar, G. *Int. J. Electrochem. Sci.* **2013**, 8, 6734.
5. Wu, J.; Xiao, Y.; Tang, Q.; Yue, G.; Lin, J.; Huang, M.; Huang, Y.; Fan, L.; Lan, Z.; Yin, S.; Sato, T. *Adv. Mater.* **2012**, 24, 1884.
6. Yamaguchi, T.; Tobe, N.; Matsumoto, D.; Nagai, T.; Arakawa, H. *Sol. Energy Mater. Sol. Cells* **2010**, 94, 812.
7. Weerasinghe, H. C.; Huang, F.; Cheng, Y. B. *Nano Energy* **2013**, 2, 174.
8. Diau, E. W. G.; Chen, C. C. (to Martine Penilla & Genarella, LLP.) U.S. Pat. 20,080,011,351 **2008**.
9. Takayasu, N. T. U.S. Pat. 20,110,284,072 **2011**.
10. Ryouji Inoue, H. S.; Shinji Yamamoto, K. S.; Keita Watanabe, O. S.; Masaaki Ishio, O. S. (to Neomax Materials Co., Ltd.) U.S. Pat. 20,130,340,820 **2013**.
11. Toivola, M.; Ahlskog, F.; Lund, P. *Sol. Energy Mater. Sol. Cells* **2006**, 90, 2881.
12. Wang, M.; Chamberland, N.; Breaux, L.; Moser, J. E.; Humphry-Baker, R.; Marsan, B.; Zakeeruddin, S. M.; Grätzel, M. *Nat. Chem.* **2010**, 2, 385.
13. Wu, J.; Lan, Z.; Hao, S.; Li, P.; Lin, J.; Huang, M.; Fang, L.; Huang, Y. *Pure Appl. Chem.* **2008**, 80, 2241.
14. Cue, G.; Guo, Y.; Yu, T.; Guan, J.; Yu, X.; Zhang, J.; Liu, J.; Zou, Z. *Int. J. Electrochem. Sci.* **2012**, 7, 1496.
15. Smestad, G. P.; Spiekermann, S.; Kowalik, J.; Grant, C. D.; Schwartzberg, A. M.; Zhang, J.; Tolbert, L. M.; Moons, E. *Sol. Energy Mater. Sol. Cells* **2003**, 76, 85.
16. Sastrawana, R.; Beierb, J.; Belledina, U.; Hemmingc, S.; Hirschd, A.; Kernd, R.; Vetterb, C.; Petrata, F. M.; Prodi-Schwabe, A.; Lechnerf, P.; Hoffmann, W. *Sol. Energy Mater. Sol. Cells* **2006**, 90, 1680.
17. Lee, K. M.; Chiu, W. H.; Lu, M. D.; Hsieh, W. F. *J. Power Sources* **2011**, 196, 8897.
18. Lee, D. Y.; Lee, W. J.; Song, J. S.; Koo, B. K.; Kim, H. J. (to Tuchman & Park LLC.) U.S. Pat. 20,080,264,482 **2008**.
19. Kishi, K.; Katsuhiko, H. *Three Bond Tech. News* **2005**, 65, 1.
20. Fukui, A.; Yamanaka, R.; Fuke, N. (to Müller-Hoffmann & Partner Patentanwälte.) Eur. Pat. 2,043,191A1 **2009**.
21. Drobny, J. G.; Moore, A. L. *Fluoroelastomers Handbook*; William Andrew: New York, **2005**; p 324.
22. Teng, H. *Appl. Sci.* **2012**, 2, 496.
23. Ebnesajjad, S. In *Applied Plastics Engineering Handbook*; Kutz, M., Ed.; Elsevier: Waltham, MA, **2011**; Chapter 4, p 49.
24. Adamson, A. W.; Gast, A. P. *Physical Chemistry of Surfaces*, 6th ed.; Wiley: New York, **1997**; p 375.
25. Emery, K. A.; Osterwald, C. R. *Sol. Cells* **1986**, 17, 253.
26. Glemser, O.; Saur, H. In *Handbook of Preparative Inorganic Chemistry*, 2nd ed.; Brauer, G., Ed.; Academic: New York, **1963**; p 1035.
27. Milinavičiūtė, A.; Jankauskaitė, V.; Narmontas, P. *Mater. Sci.* **2011**, 17, 378.
28. Leadley, S.; O'Hare, L. A.; McMillan, C. In *Silicone Surface Science*; Owen, M. J., Dvornic, P. R., Eds.; Springer: New York, **2012**; Chapter 12, p 319.